AFRL-PR-WP-TR-2006-2228

ULTRA HIGH WORK, HIGH EFFICIENCY TURBINES FOR UAVs

Rolf Sondergaard

Turbine Branch (AFRL/PRTT)
Turbine Engine Division
Propulsion Directorate
Air Force Materiel Command, Air Force Research Laboratory
Wright-Patterson Air Force Base, OH 45433-7251

JUNE 2006

Final Report for 01 January 1997 – 31 March 2005

PROPULSION DIRECTORATE
AIR FORCE MATERIEL COMMAND
AIR FORCE RESEARCH LABORATORY
WRIGHT-PATTERSON AIR FORCE BASE, OH 45433-7251

NOTICE AND SIGNATURE PAGE

Using Government drawings, specifications, or other data included in this document for any purpose other than Government procurement does not in any way obligate the U.S. Government. The fact that the Government formulated or supplied the drawings, specifications, or other data does not license the holder or any other person or corporation; or convey any rights or permission to manufacture, use, or sell any patented invention that may relate to them.

This report was cleared for public release by the Air Force Research Laboratory Wright Site (AFRL/WS) Public Affairs Office and is available to the general public, including foreign nationals. Copies may be obtained from the Defense Technical Information Center (DTIC) (http://www.dtic.mil).

AFRL-PR-WP-TR-2006-2228 HAS BEEN REVIEWED AND IS APPROVED FOR PUBLICATION IN ACCORDANCE WITH ASSIGNED DISTRIBUTION STATEMENT.

*//Signature//
Dr. Rolf Sondergaard
AFRL/PRTT

//Signature//
Charles W. Stevens
Chief, AFRL/PRTT

//Signature//
JEFFREY M. STRICKER
Chief Engineer
Turbine Engine Division
Propulsion Directorate

This report is published in the interest of scientific and technical information exchange, and its publication does not constitute the Government's approval or disapproval of its ideas or findings.

*Disseminated copies will show "//Signature//" stamped or typed above the signature blocks.

REPORT DOCUMENTATION PAGE

Form Approved
OMB No. 0704-0188

1. REPORT DATE *(DD-MM-YY)*	2. REPORT TYPE	3. DATES COVERED *(From - To)*
June 2006	Final	01/01/1997 – 03/31/2005

4. TITLE AND SUBTITLE
ULTRA HIGH WORK, HIGH EFFICIENCY TURBINES FOR UAVs

5a. CONTRACT NUMBER
In-house

5b. GRANT NUMBER

5c. PROGRAM ELEMENT NUMBER
61102F

6. AUTHOR(S)
Rolf Sondergaard

5d. PROJECT NUMBER
2307

5e. TASK NUMBER
NP

5f. WORK UNIT NUMBER
01

7. PERFORMING ORGANIZATION NAME(S) AND ADDRESS(ES)

Turbine Branch (AFRL/PRTT)
Turbine Engine Division
Propulsion Directorate
Air Force Materiel Command, Air Force Research Laboratory
Wright-Patterson Air Force Base, OH 45433-7251

8. PERFORMING ORGANIZATION REPORT NUMBER
AFRL-PR-WP-TR-2006-2228

9. SPONSORING/MONITORING AGENCY NAME(S) AND ADDRESS(ES)

Propulsion Directorate
Air Force Research Laboratory
Air Force Materiel Command
Wright-Patterson AFB, OH 45433-7251

10. SPONSORING/MONITORING AGENCY ACRONYM(S)
AFRL-PR-WP

11. SPONSORING/MONITORING AGENCY REPORT NUMBER(S)
AFRL-PR-WP-TR-2006-2228

12. DISTRIBUTION/AVAILABILITY STATEMENT
Approved for public release; distribution is unlimited.

13. SUPPLEMENTARY NOTES
PAO case number: AFRL/WS 06-1380; Date cleared: 31 May 2006. This report contains color.

14. ABSTRACT

The opportunity for the reattachment and control of separated flows occurs in inlets, compressors, transition ducts and turbines. Passive and active control of separated flows has been demonstrated successfully by a number of techniques which employ the introduction of longitudinal or streamwise vortices. The role of these vortices is initially to reenergize the wall boundary layer flow by entraining and redistributing momentum from the primary flow to the wall layer and enhance early transition. A chain of non-linear interactions of these unsteady vortices with large scale unsteady separation vortices and the shed shear layer results in significant alteration of the circulation. The resulting increased circulation allows higher blade loadings, reduced part count, and improved performance at low Reynolds numbers.

15. SUBJECT TERMS
Low pressure turbine, turbine separation control, turbine loading

16. SECURITY CLASSIFICATION OF:			17. LIMITATION OF ABSTRACT:	18. NUMBER OF PAGES	19a. NAME OF RESPONSIBLE PERSON (Monitor)
a. REPORT	b. ABSTRACT	c. THIS PAGE			Rolf Sondergaard
Unclassified	Unclassified	Unclassified	SAR	32	19b. TELEPHONE NUMBER *(Include Area Code)* N/A

TABLE OF CONTENTS

List of Figures....iv
Abstract....v
Acknowledgments....vi
Introduction....1
Separation of Low Pressure Turbines at Low Reynolds Numbers....1
Separation Control Techniques....3
Forcing Frequencies....3
Experimental Setup....6
Results....8
Dimple Vortex Generators....8
Comparison with Computations, Dimples....11
Continuous and Pulsed Vortex Generator Jets....13
Blade Profile and Total Inlet Pressure Measurements....14
Summary....16
References....18
Nomenclature....22

LIST OF FIGURES

Figure 1. VBI calculation of loss Coefficient for Pak B compared with experimental measurements

Figure 2. Comparison of mid passage and end wall losses from Matsunuma et al., 1998

Figure 3. Heater configurations, CL, and CD, 2˚ increase in maxium angle of attack with thermal vorticies

Figure 4. Cascade tunnel test section.

Figure 5. Dimpled blade, dimples @ 55%, 60%, & 65% Cx / VGJ blade, 90˚ skew, 30˚ pitch VGJ's @ 45, 63% C_x

Figure 6. c_p profiles: VBI at Re=100k and baseline measurements at Re= 25K, 50K, 100K

Figure 7. Shear layer & wake traverse locations.

Figure 8. Hot wire boundary layer micro traverses Re = 25K, baseline

Figure 9. Wake loss coefficient, Re= 25K, 50K, 100K.

Figure10. (a) Dimple cavity flow schematic (b) visualization, a) at 90°, b) at 135° , c) at 225° measured from the primary flow direction from Mahmood et al., 2000

Figure 11. Dimpled blade loss coefficient for Tu = 1%.

Figure 12. Dimpled blade loss coefficients for Tu = 4%

Figure 13. Mach number comparison of Pak B with/without dimple from MISES by Koch.

Figure 14.Comparison of wake losses for (a) 2.22 and (b) 4.44 cm span wise dimple spacing.

Figure 15. Loss coefficients for steady VGJ control (a) as function of blowing ratio (b) as function of Re

Figure 16. Pulse width measurements at the VGJ exit, 10Hz, 63% Cx, Re=25,000.

Figure 17. Mid boundary layer power spectral density@ 68%Cx, VGJ at 63% Cx, Re = 25,000.

Figure 18. (a) Velocity boundary layer profiles for pulsed VGJ's. (b) Turbulence profiles for pulsed VGJs.

Figure 19. (a) Loss coefficient for pulsed VGJ's, Tu =1%, Re = 25,000. (b). Loss coefficient vs forcing f.

Figure 20. No control separated flows, pitch 1.5.

Figure 21. VGJ reattachment with increasing pitch, S.

Figure 22. Design vs as fabricated cascade profile < ±0.25mm.

Figure 23. Dimpled HP vanes.

ABSTRACT

This is a summary of the work performed under Job Order Number 2307NP01. This was an in-house task funded under AFOSR ILIR grant 97WL003N07.

The opportunity for the reattachment and control of separated flows occurs in inlets, compressors, transition ducts and turbines. Passive and active control of separated flows has been demonstrated successfully by a number of techniques which employ the introduction of longitudinal or streamwise vortices. The role of these vortices is initially to reenergize the wall boundary layer flow by entraining and redistributing momentum from the primary flow to the wall layer and enhance early transition. A chain of non-linear interactions of these unsteady vortices with large scale unsteady separation vortices and the shed shear layer results in significant alteration of the circulation. The resulting increased circulation allows higher blade loadings, reduced part count, and improved performance at low Reynolds numbers. Passive dimples with single and multiple rows, varied dimple location and dimple shape have been investigated. Active Vortex Generator Jets (VGJs), both steady flow and pulsed flow, at a variety of injection locations have also been investigated. Initial studies of a single row of dimples and their wakes on a high Mach number, high pressure turbine vane ring have been performed at Reynolds numbers down to 13,500 in a full scale matched parameter rig. Properly placed dimples or VGJs help reattach separated flows at all Reynolds numbers investigated. Computations for the dimple geometries with VBI, MISES, and Fluent have been carried out to determine initial separation, compressible implications, reattachment locations, and predicted wake profiles and loss coefficients.

Acknowledgments

This work was preformed under the sponsorship of The Air Force Office of Scientific Research, Dr Thomas Beutner program manager. James Lake, Kurt Rouser, and John Casey are Air Force Institute of Technology Ph.D. and Masters Students who carried out their experimental work in the Propulsion Directorate's low Reynolds number cascade facility.

INTRODUCTION

Separation of Low Pressure Turbines at Low Reynolds Numbers

The losses encountered by highly loaded low pressure turbines operating in the axial chord Reynolds Number range of 10,000 to 100,000 can seriously limit both turbine efficiency and work output, thus decreasing the available power and increasing the specific fuel consumption of the engine. Figure 1 compares a calculation of turbine loss coefficient using the Vane Blade Interaction (VBI) code with experimental values at two free-stream turbulence levels. The large increase in losses at low Re is due to massive separation of the suction side boundary layer. Separation is observed to occur near the location where uncovered turning (flow expansion outside of the turbine passage) begins.

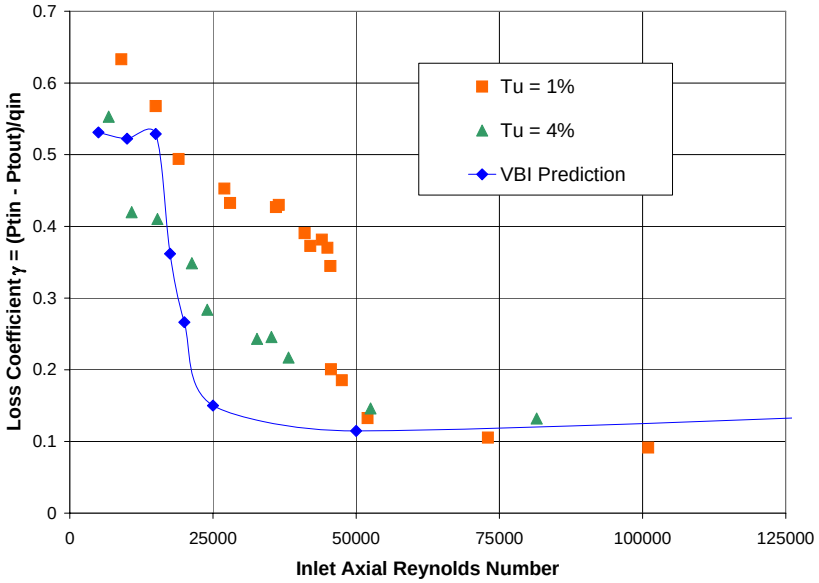

Figure 1. VBI calculation of loss Coefficient for Pak B compared with experimental measurements.

Significant differences between measurement and computation exist in the low Reynolds number range. This is primarily due to the inadequacies of the computational model in predicting separation onset (hence the missed location of the loss "knee") and transition after separation occurs (the abrupt transition from low loss to high loss in the computation compared to the more gradual change in the experimental measurements). The effect of turbulence is seen in Figure 1 to have little effect on the separation onset Reynolds number, but makes the losses grow more gradually as Reynolds number drops. This is due to the enhanced transition and hence the existence of flow reattachment at moderate Reynolds numbers for the experimental results.

The consequence of separation is a decrease in overall turbine efficiency of 4-6% (Helton, 1997)[1] as the Reynolds number drops below 100,000. The separation losses are even more severe in the end wall regions where they are nearly twice the mid span losses, as illustrated in Figure 2[2]. The efforts at boundary layer control have continued to

evolve over the last decade and the possibility of effective separation control has been demonstrated in a number of experiments.

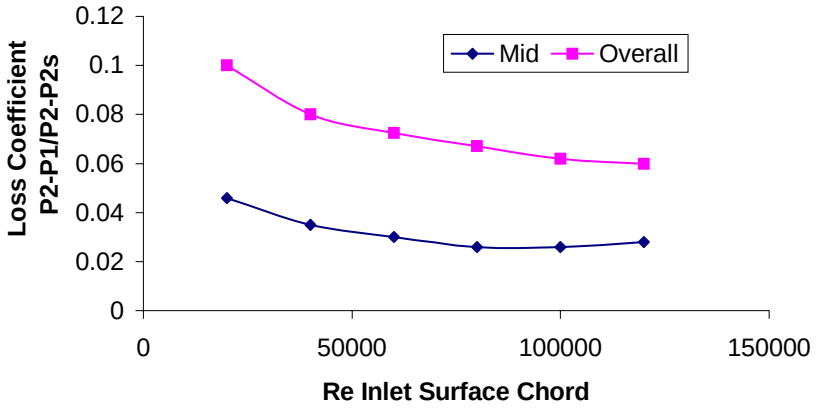

Figure 2. Comparison of mid passage and end wall losses from Matsunuma et al., 1998.

Several efforts have been made to document and improve the computation of turbine flows under the low Reynolds number conditions encountered in the LPT. Computational and experimental efforts to define and model these flows included Dorney and Ashpis, Qui and Simon, Sohn et al., and Huag and Xiong, [3-6], among others. Extensive measurements of heat transfer, transition, separation, and boundary layer profiles, as a function of turbulence, turbulence scale and Reynolds number have been obtained in a Langston turbine cascade at Reynolds numbers down to 38,000 at the US Air Force Academy[7]. Huanag et al., List et al., and Hultgren et al., [8-10] have demonstrated reattachment of separated Pack B (an experimental Pratt & Whitney blade design) cascade or simulated Pack B cascade flows using atmospheric glow discharge plasmas.

Another technique which has demonstrated success has evolved from the work of Halstead et al. [11,12], in which turbulent spots were observed to be followed by a becalmed regions where the flow is laminar and no further turbulent bursts occur. Howell et al., and Arts and Coton[15-17]employed this technique with the superposition of wakes to reduce LPT separation losses on highly loaded turbine blades. The physical process at the wall (the creation of a becalmed region) may be similar to what is taking place with pulsed vortex generator jets, synthetic jets, electrostatic devices, and rapid transverse strain.

Three successful techniques of separation control have now been demonstrated under this project in a highly loaded LPT cascade at the Air Force Research Laboratory. The performance of the LPT dimples, the steady VGJ's, and the pulsed VGJ's will be summarized in terms of loss coefficients as a function of Reynolds number. The separation has been effectively controlled in all cases with unchanged losses at higher Reynolds numbers. In addition to reducing the losses the loading can now also be significantly increased.

Separation Control Techniques

Nearly all separation control techniques involve the introduction of longitudinal or streamwise vortices in some form. Studies into such techniques go back over fifty years[17]. Some of the most well known passive generation techniques include: half delta wings or fences, which are currently extensively employed on external aircraft flows; riblets [18] employed primarily on external flows to increase heat transfer; dimples[19-22] employed on golf balls; Large Eddy Breakup Devices (LEBU's); roughness; turbulent trips[18,23]; and "micro dots" [24]. Active techniques include: naturally lifted flaps on sailplane wings [25]; actively forced flows[23]; blown flaps[26,27]; suction or blowing [28]; thermal riblets,[29]; synthetic jets [6,30-33]; surface deformation [33]; electrostatic and plasma interactions with flows [34-38]; rapid transverse strain [39,40]; acoustic cavities or acoustic forcing; electromagnetic flow interactions; and MEMS devices employing various combinations of the previous techniques.

Study of steady and non steady blowing on flaps and slots on wings and in diffusers has been underway for a number of years as well. Nagaraja, [41] summarizes the history of ejector and blown flap work that took place at Wright Patterson in the 1960's and 1970's for V/STOL applications. Thrust augmentation of a factor of two was demonstrated and several blown wings were developed for very high lift "super circulation" effects and increased angle of attack possibilities were recognized from the application of ejectors to airfoils.

Much of the current separation control and drag reduction work originated in the 1980's with the non steady trapping and control of vortices on pitching wings to mimic birds flight at high angles of attack. Meyer, et al., [24], in their glider work to increase lift and useful angle of attack, employed passive flaps, which lifted like birds feathers when stall or separation occurred effecting a passive reattachment of the separated flow. Meyer evaluated several combinations of lifting flaps and vortex generators on a sail plane airfoil operating at Reynolds number near one million. Lift coefficient increases of 25% to 40% were demonstrated. Meyer noted that approximately equal improvements came from the passive flaps and the introduction of longitudinal vortices. The introduction of longitudinal vortices then followed on axi-symmetric bodies and delta wings by riblets and their derivatives to mimic biological observations of marine species[42]. Riblets showed drag reductions of 6-8% [18]. The riblets also showed a 6-8% reduction in heat transfer in the presence of free stream turbulence of 8-10% in a turbine cascade[43]. Laser velocimetry measurements have shown the principal flow structures resulting from riblets to be a system of longitudinal vortices[44]. The observation that riblets continue to function in the presence of turbulence indicated that the longitudinal vortices could be an effective mechanism for reattachment of separated turbulent LPT flows, which are typically high turbulence environments.

Forcing Frequencies

Using a compressible 2D NS solver Wu et al., [28] showed up to 70% increases in non steady airfoil lift for effective forcing frequencies of 0.3 to 2.0*f_{shed} at Reynolds numbers of $5x10^5$. Weaver et al.[27] found a 12% lift increase from steady suction / surface blowing and a 20% increase from pulsed blowing with an F+ of 0.9 and Cμ's of 0.19 to 0.56. Another separation control technique which has been successful is the "synthetic jet"[30,45,46]. The synthetic jet

is a wall cavity driven by a diaphragm in the bottom of the cavity. This is a zero net mass flow device which drives a high momentum starting jet through the boundary layer into the primary flow, then draws a low momentum flow back into the cavity as the diaphragm retracts to its starting position. This device has been used to produce effective control of separated flows on cylinders and on a simulated unbounded airfoil by actuation at the leading edge. This technique is thought to alter the apparent boundaries and streamlines by changing the bounded circulation of the flow by the starting and stopping vortices.

Wygnaski and Seifert[26] experimentally, and Fasel[47] computationally observed in their Wall Jet work that the same level of skin friction reduction was found for non steady wall jet flows with a low duty cycle as with continuous wall jet flows. Wygnaski's observations indicated that the starting / stopping vortices play an important role in the near wall flow stability and the entrainment of free stream fluid. Wygnaski estimated the optimum forcing frequency to prevent separation on a blown flap to be given by the size of the separation bubble or the flap deflection and the reduced frequency $F+ = fL_f/U_\infty \sim 1$ with a phase velocity of 0.5. For an air foil, Nagib et al., [48], found the optimum F+ based on chord to be between 1 and 3. This nominal value of 1 of reduced frequency is equivalent to that found by Amity et al., [31] as well as Glezer [30]. The impact of the starting and stopping vortices on the near wall flow is substantial, since these vortices are nearly always an order of magnitude stronger than the following steady shear layer vortices. This is reinforced further by the observations by Glezer when comparing pulsed injection to a sinusoidal injection of the same frequency. The sinusoidal injection was found ineffective in promoting any change to a separated flow, while the pulse injection at the same frequency effected reattachment.

The above devices and techniques all have a common span wise pressure distribution which is periodic. Driver et al., [39] showed that turbulence production is suppressed when a flow is subjected to a sudden transverse strain. Jung et al., [40] studied the suppression of turbulence with span wise oscillations of a wall bounded flow using a DNS computation. They found they could reduce turbulent drag by 10-40% by suppressing wall turbulence for non dimensional ($T^*u_\tau^2/\nu$) oscillation periods of $25<T_{nd}<200$. When the flow oscillation was replaced by an oscillating wall, only the flow near the wall was affected. Thus a distributed oscillation across the flow field is required to affect or control the flow. This pressure distribution can be produced by many techniques including fluidic, mechanical, thermal, acoustical, or electro-magnetic.

Yurchenko, et al.[29], in studying the stability of boundary layer flows and Görtler vortices, found that stable longitudinal vortices could be introduced into the flow in the near wall region if one chose a frequency or scale smaller than the fundamental most unstable frequency using external vortex generators. Stable or long lived vortices are expected with experimental points for concave and convex curvature for the scale size parameter $\Lambda o \sim U_\infty/\nu \, (\lambda_z^3 / R)^{0.5} > 39$. Saric et al.,[23], has also used this rational to scale the micro dots used to create the longitudinal vortices which have demonstrated increases of ~60%, in the laminar flow regions on a swept unbounded airfoil with low free stream turbulence. Saric used micro dots of a size and spacing less than the most unstable mode of the flow. The

parameter range for stable long lived vortices is quite large and compatible with the favorable interactive frequencies or scales of the Wu et al.[20] study.

Yurchenko et al.[29] investigated thermally excited longitudinal vortices with chord wise heating elements at some 20 location configurations and two span wise spacings around an unbounded airfoil. The large number of configurations was achieved with a symmetric reversible airfoil. Temperature deltas of up to ~ 20˚ C were employed to generate the thermal vortices which allowed an increase of 2˚ in the maximum angle of attack and an increase in the lift/ drag ratio for this special airfoil as illustrated in Figure 3. The leading edge of the suction surface was found to be the most effective location of the heaters.

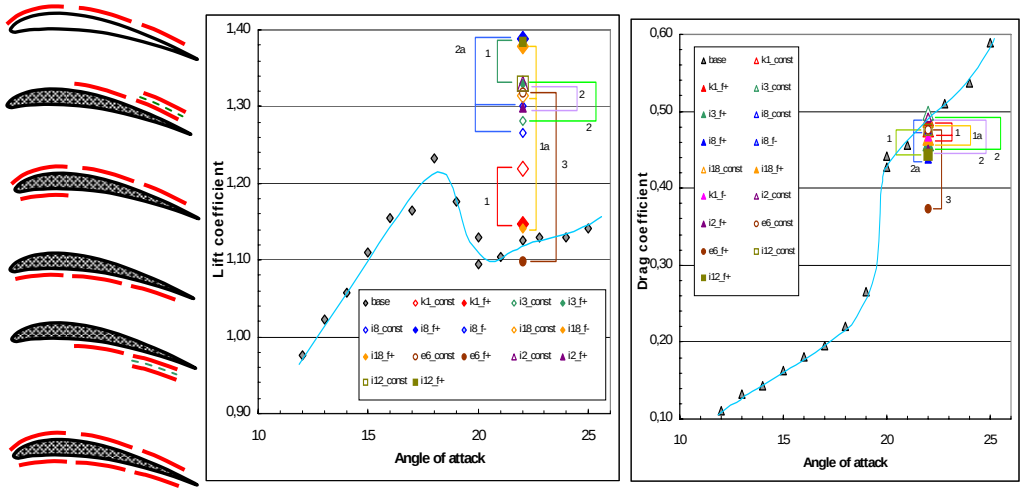

Figure 3. Heater configurations, CL, and CD, 2˚ increase in maxium angle of attack with thermal vorticies.

Previous work has shown longitudinal vortices are clearly effective in suppressing the wall generation of turbulence and estimates can be made of the scale size, location, and appropriate reduced frequency for effective application. The design space seems to be quite large from Yurchenko's and Wu's work and these estimates are supported by a number of experimental studies.

The object of highly loading the blading is to reduce the number of blades to do the same amount of work, thereby reducing the weight of the LPT. Howell et al. and Arts and Coton, [15-17] estimated that a 34% reduction in blade count (LPT weight) can be effected over current LPT's with a highly loaded LPT.

The Low Pressure Turbine (LPT) Low Reynolds number problem is in a Reynolds number range where many of these techniques can be particularly effective. The low pressure turbine must also operate well at high Reynolds numbers (take off and low altitudes) without incurring significant additional losses. The results of applying a Dimple technique, pulsed, and steady skew vortex generator jets to separation control for the LPT will be described in the following sections. Current results from dimple computations and the application of dimples to HPT vanes in an annular cascade operating at low Reynolds numbers will be presented.

EXPERIMENTAL SETUP

The cascade tunnel used in the experiments is an open circuit induction tunnel. The test section (0.85m by 1.22m) is shown schematically in Figure 4. It has 9 PackB profile blades (Figure 5) with chords of 17.78 cm and an aspect ratio of 4.92. The inlet flow angle is 35± 2˚, the exit flow angle is 60˚± 2˚, as measured by a 30˚ three-hole wedge probe[50]. These blades are highly aft loaded and tend to strongly separate at low Reynolds numbers. The typical loss coefficient obtained from VBI computations was shown in Figure 1 for this cascade. The problem is that the loss coefficient and the Reynolds number at which the losses rise steeply are very dependent on the prediction of transition and separation in a non steady flow. This still remains an elusive and inaccurate computation as is illustrated by the factor of 2 to 4 difference between experiment and theory.

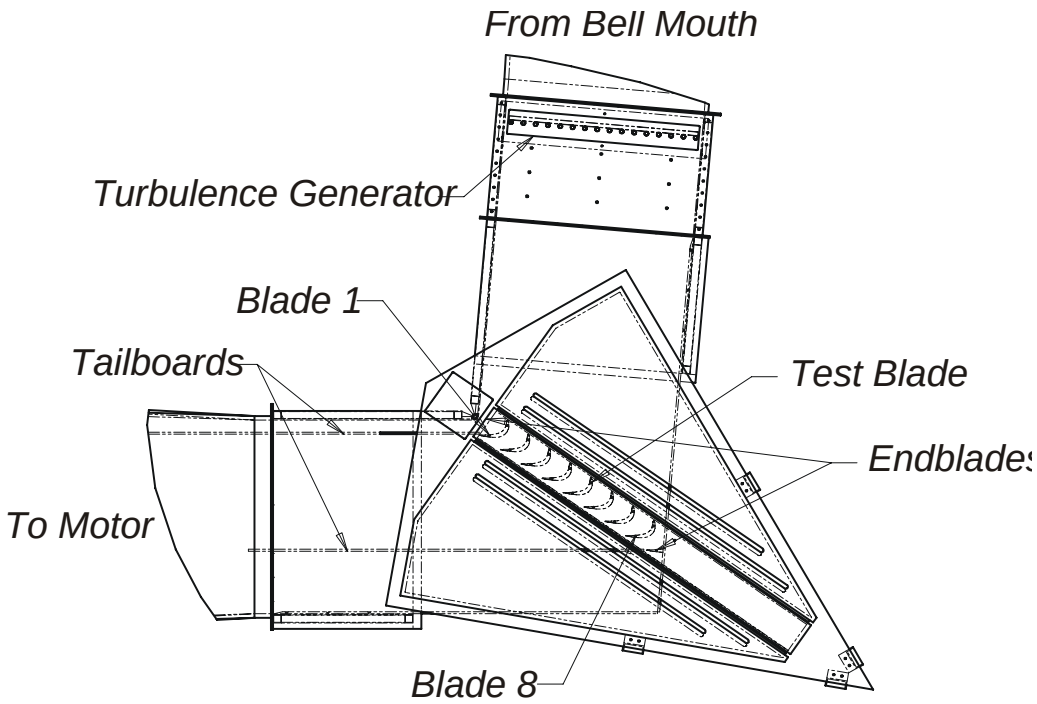

Figure 4. Cascade tunnel test section.

The same tunnel and cascade is used for both the dimple and the vortex generator jet separation control experiments. With the cascade installed the tunnel is capable of producing uniform velocities of 3-60m/sec ± 0.1m/sec with uniform free stream turbulence less than 1% at the test section entrance. Higher turbulence levels are introduced by a rectangular mesh with a spacing of 7.5 cm between round tubes of 2.5 cm diameter. The grid is located 10 axial chords upstream of the cascade. The cascade is located well into the final period of decay at 92 tube diameters downstream of the grid. The grid generates a uniform, turbulence level of 4% ± 0.3%, with an integral length scale of 2.5cm, typical of LPT conditions [9], at the entrance to the cascade. Blades 4, and 6 are instrumented with 40

pressure taps each, blade 5 (the active/passive control blade) has 19 taps to provide detailed cp distributions for all test conditions. Baseline cp distributions are shown in Figure 6 at Re=25K, 50K and 100K. Hot wire boundary layer traverses are typically obtained at 12 stations (Figure 7) between 63% C_x and the trailing edge as illustrated in Figure 8 which shows separation occurring between 73% and 75% C_x at a Re of 25K. Loss coefficients are obtained from integration of the wake loss profile 0.64 axial cords downstream of the trailing edge of the blade as illustrated in Figure 9. The accuracy of the hot wire velocity measurements was determined to be ±2%, c_p ±0.18, and the loss coefficient ±8%.

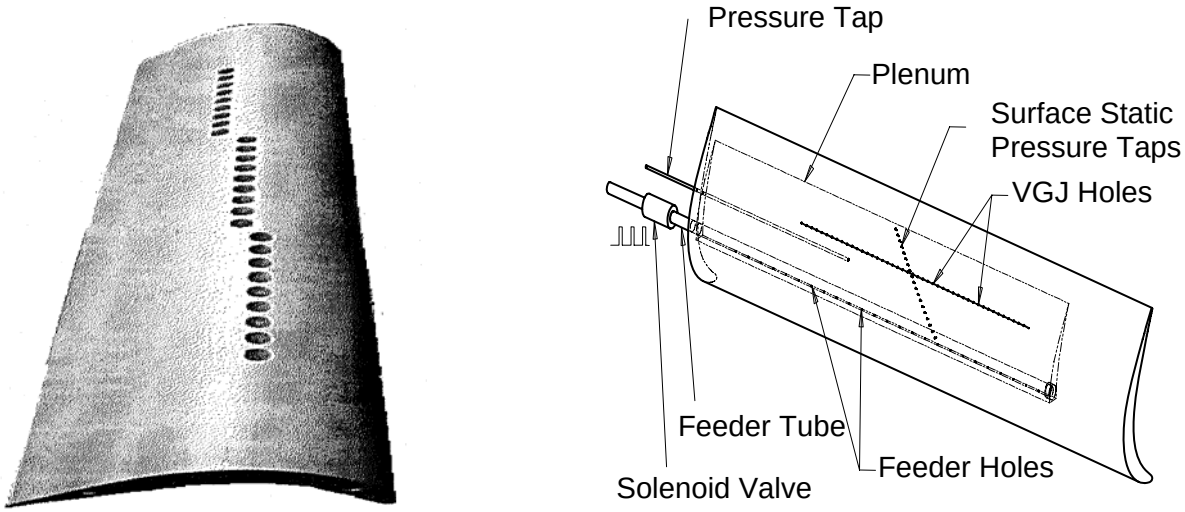

Figure 5. Dimpled blade, dimples @ 55%, 60%, & 65% Cx / VGJ blade, 90˚ skew, 30˚ pitch VGJ's @ 45, 63% C_x.

codes.

Figure 6. c_p profiles: VBI at Re=100k and baseline measurements at Re= 25K, 50K, 100K.

Error! Objects cannot be created from editing field

Figure 7. Shear layer & wake traverse locations.

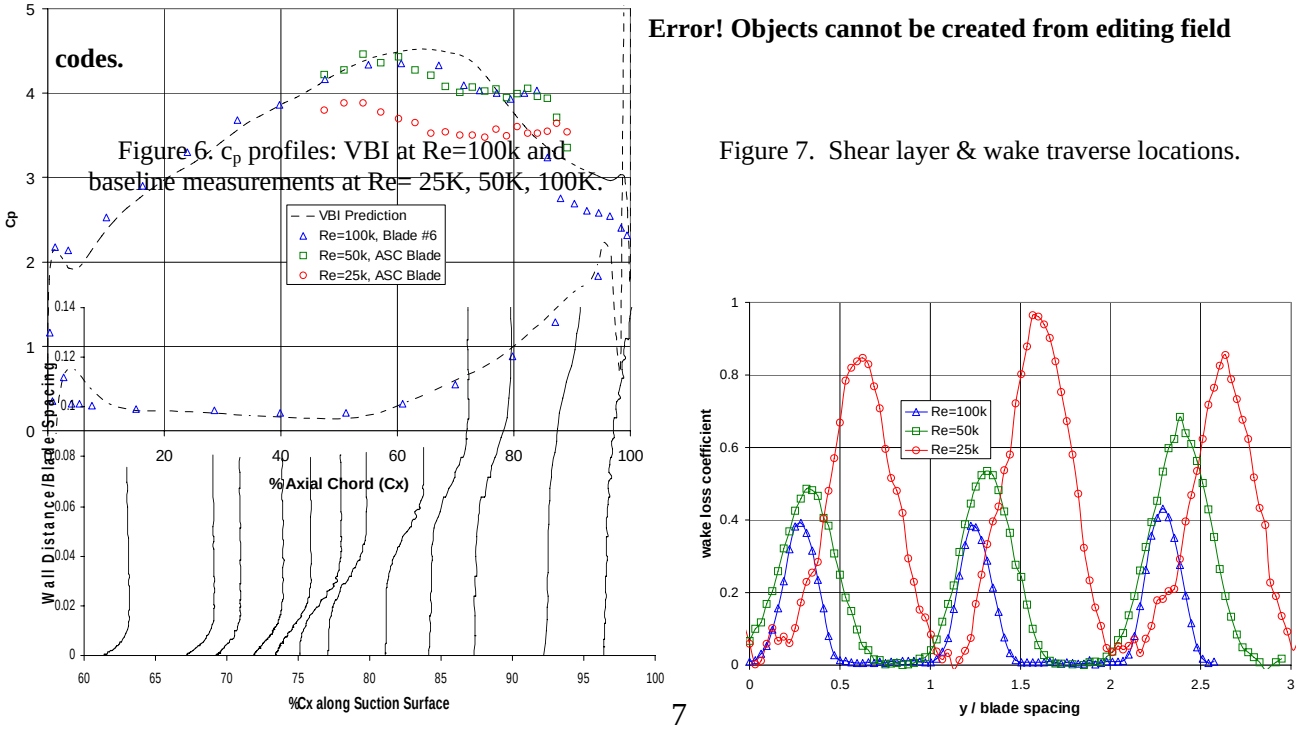

Figure 8. Hot wire boundary layer micro traverses Re = 25K, baseline.

Figure 9. Wake loss coefficient, Re= 25K, 50K, 100K.

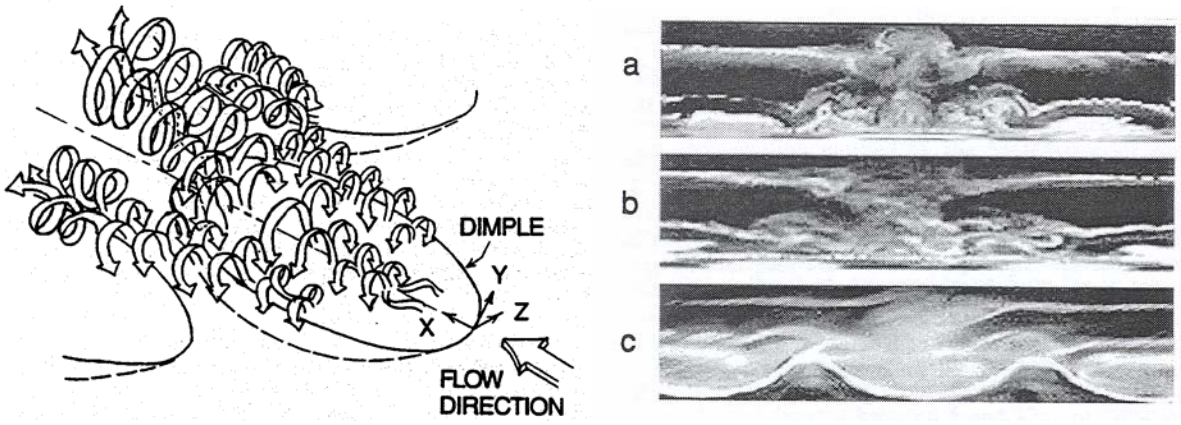

Figure10. (a) Dimple cavity flow schematic (b) visualization, a) at 90°, b) at 135° , c) at 225° measured from the primary flow direction from Mahmood et al., 2000.

RESULTS

Dimple Vortex Generators

Experimental measurements of the transition and separation locations were obtained with miniature hot wire measurements of boundary layer profiles for Reynolds numbers ranging from 25,000 to 172,000. Separation occurred between 62% and 75% chord for 1% free stream turbulence, and at 75 to 77% chord for 4 % free stream turbulence. Free stream turbulence clearly moves the separation rearward and reduces the separation length. Dimples have long been employed on golf balls. More recently heat transfer, and pressure drop measurements, and flow visualization[21,22,49] have been used to explore and document the physical flow mechanisms which result from flow over and in dimples. Flow visualization from Mahmood et al.,[21] shows a system of three longitudinal vortex pairs being shed from a round dimple cavity in an array (channel Re =1250 and channel height to dimple depth 0.5), Figure 10. Lake, [50], used the empirical relationship employed for golf ball dimples from the testing of Bearman and Harvey,[19,20], to modify a blade surface in the cascade with a single row of span wise 22.2 mm spaced dimples. The dimples have a depth to diameter ratio 0.009, giving them a depth of 1.59 mm. The depth is very close to the measured boundary layer thickness at 67% chord at Re = 43K. These dimples have an elliptical shape due to the blade curvature. Lake evaluated three dimple locations, (50% C_x), (60% C_x), and (65% C_x) as shown in Figure 5.

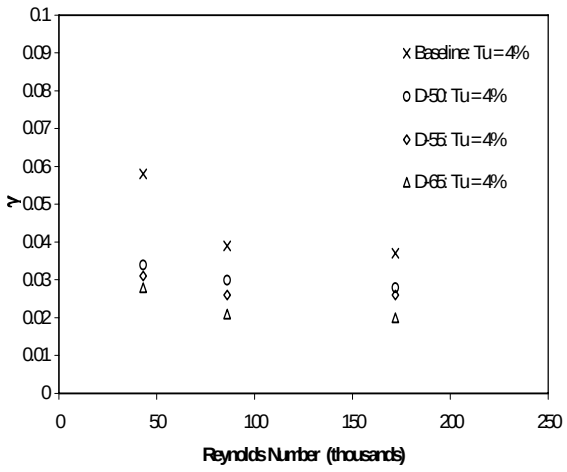

Figure 11. Dimpled blade loss coefficient for Tu = 1%.

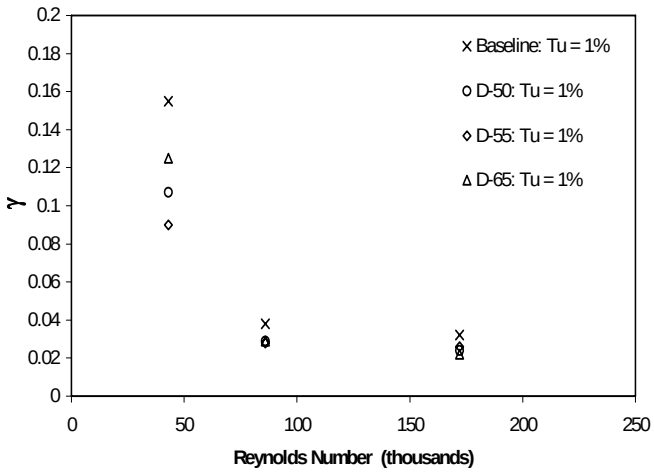

Figure 12. Dimpled blade loss coefficients for Tu = 4%.

The loss coefficients $\gamma = (p_{T,in}-p_{T,ex})/(p_{T,in}-p_{S,in})$ for each configuration are shown in Figure 11 for Tu=1% and Figure 12 for Tu=4%. The effect of turbulence on the baseline blading is to move the separation/transition rearward and decrease the size and length of the separation bubble. For 4% Tu the largest effective reduction in loss coefficient (45-50%) is consistently achieved with the 65% dimple location for all Reynolds numbers tested. Separation occurs at ~75% C_x for all Tu=4% cases, so this is always the closest location to separation. Even at the highest Reynolds numbers there is still a reduction in the loss coefficient with the addition of dimples. It is noteworthy that the dimples don't have to be located precisely at the separation location to be effective.

In contrast to the work of Wu et al., and Yurchenko et al.,[28], on unbounded airfoils where control is initiated near the leading edge (2.5% chord), the placement of the dimples, and the vortex generator jets, in the current work is very close to the natural separation point. The dimples and vortex generator jets are even effective when placed after the natural separation location, but most effective before separation.

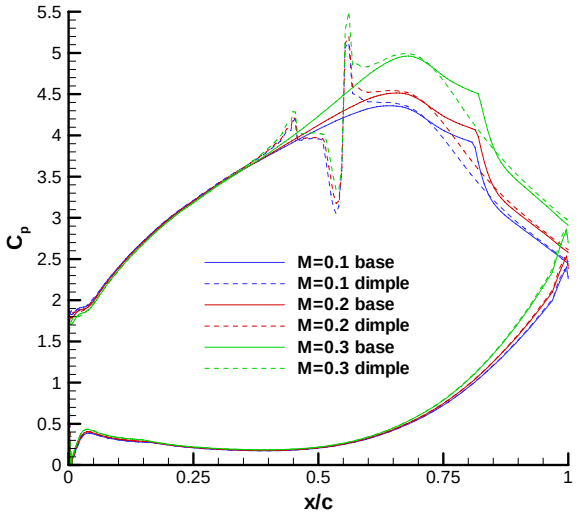

Figure 13. Mach number comparison of Pak B with/without dimple from MISES by Koch.

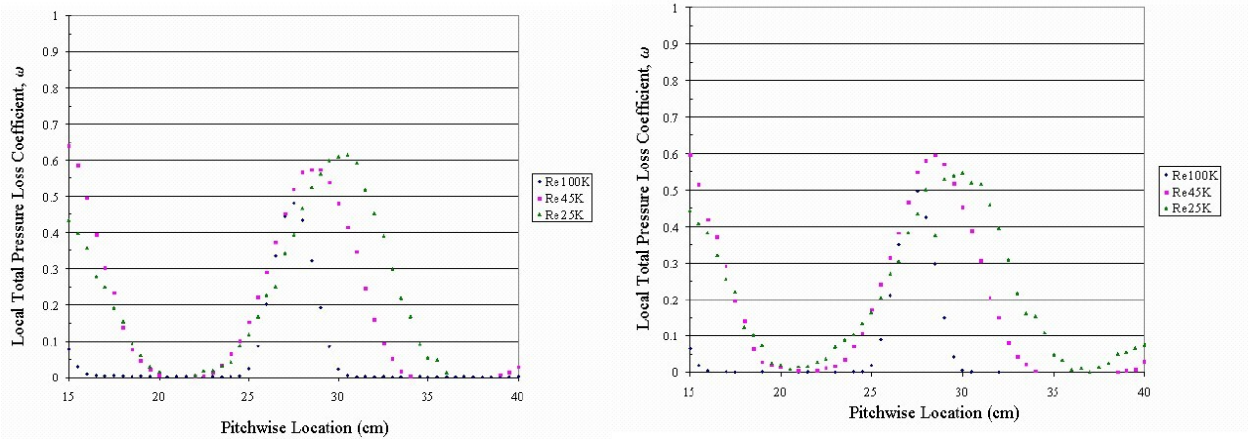

Figure 14.Comparison of wake losses for (a) 2.22 and (b) 4.44 cm span wise dimple spacing.

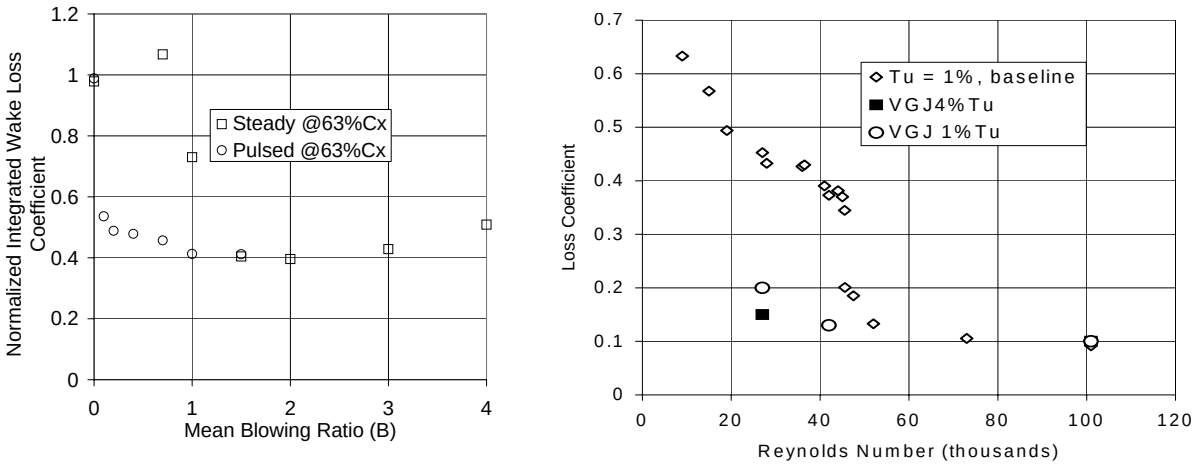

Figure 15. Loss coefficients for steady VGJ control (a) as function of blowing ratio (b) as function of Re.

Comparison with Computations, Dimples

VBI, a steady DNS solver was initially used to predict the location of separation of the untreated blade. Separation was found to occur at approximately the location of uncovered turning with small movement with Re and turbulence intensity and this was subsequently confirmed experimentally. MISES, a steady 2D Reynolds averaged solver, was used by Koch[51] to examine the effect of compressibility on both the clean and dimpled blade. Koch studied Mach numbers from .06 to 0.3 with separation initiated near the uncovered turning location for the undimpled blade. Dimples were located just ahead of the uncovered turning and reattachment was effected for all Mach numbers for the dimpled configurations, Figure 13.

Rouser[51], and Casey[52], used unsteady 3D Fluent in laminar mode to examine the separation / reattachment locations, wake loss, and vortex shedding of the Pak B cascade. Laminar mode (no turbulence model) was required because Fluent failed to show separation in the desired range of Re using K-ω, K-ε, or Spalart-Allamaras. turbulence models. The turbulence models transitioned too early and over-stabilized the computational boundary layers.

Rouser and Casey examined the Pak B cascade with and without dimples for Re's of 25K, 45K, and 100K. Local experimental boundary layer profiles are typically obtained at 67.2% C_x, 73% C_x, 79.3% C_x, 84.8% C_x, and 89.9% C_x with single and double hot wire probes. The undimpled blade is observed from boundary layer profiles to separate at <0.73% C_x at a Re of 25K, < 79% at a Re of 45K and < 89.8% at a Re of 100K. The loss coefficient γ, is determined by wake traverses at blade span wise centerline in the exit plane at -0.67 C_x and up stream at approximately +2 C_x.

The original dimple spacing used by Lake was based on the Gortler vortex diameter and Gortler stability criteria; however there had been no specific experimental or computational investigation at that time to examine if this was the best choice. Asymmetric dimples are known to shed larger numbers of vortices so it would be desirable to know what the improvement might be for increasing the complexity of the dimple shape. Rouser examined filling in one half of the span wise dimples on Lake's blade, with dimples at 50%, 55%, and 65% C_x, finding both experimentally and computationally that this configuration actually shed fewer vortex pairs and was not as good as the original asymmetric elliptical dimple shape of Lake. Casey, followed with doubling the span wise spacing of dimples, comparing spacings of 2.22 and 4.44 cm. The wake loss profiles for 2.22 and 4.44 cm span wise spacing of the dimples are shown in Figure 14 and can be seen to be nearly identical. This implies that the span wise influence of the dimples is considerably larger than originally anticipated. The picture which emerged from the computations, at a Re of 25K, using laminar Fluent was that of a separation occurring at 66% C_x with two successive reattachments and a boundary layer 12 mm thick at 89.9% C_x. The reattachments represented pairs of bound vortices. The unsteady computational separation oscillated between 64.5% and 68.5% C_x at a frequency of 11 Hertz. For the 25K Re case, with dimples at 60% C_x, a small separation occurred computationally at 73% C_x with many smaller mixed local separations and reattachments and a resulting large decrease in the shed wake. The 4.44 cm span wise dimple

spacing computationally separated at 71%. The 4.44 cm span wise spacing computationally achieved a better loss coefficient reduction for a single row of dimples with a 68% reduction in loss coefficient versus 58% for the 2.22 cm spacing. Experimentally the 2.22 and 4.44 cm dimple spacing loss coefficient was the same within the experimental uncertainty. Casey also examined a single dimple row at 65% C_x and two rows of dimples at 65% and 76% C_x with span wise dimple spacing of 2.22 and 4.44 cm. The 2 rows of dimples computationally had a 63% reduction in loss coefficient. The single row again proved to be the better configuration both computationally and experimentally.

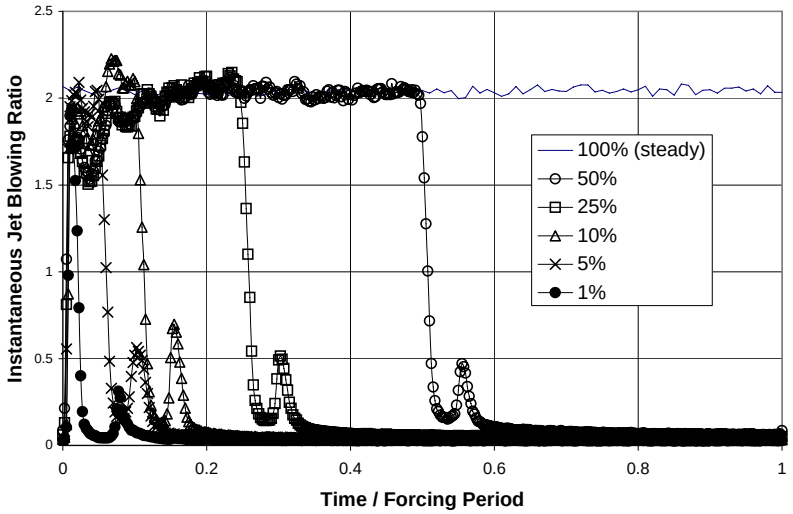

Figure 16. Pulse width measurements at the VGJ exit, 10Hz, 63% Cx, Re=25,000.

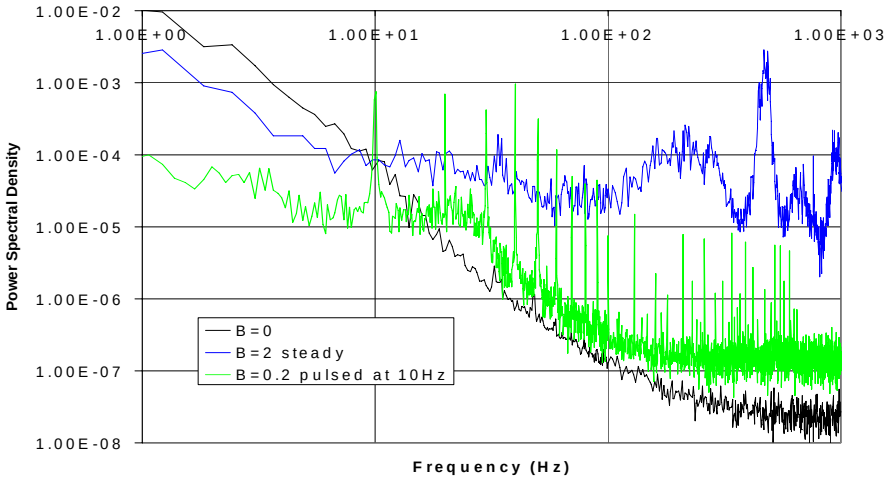

Figure 17. Mid boundary layer power spectral density@ 68%Cx, VGJ at 63% Cx, Re = 25,000.

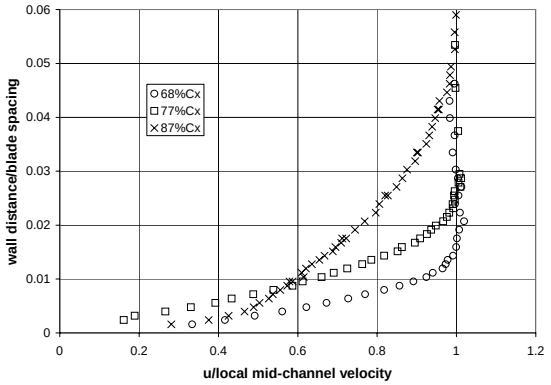

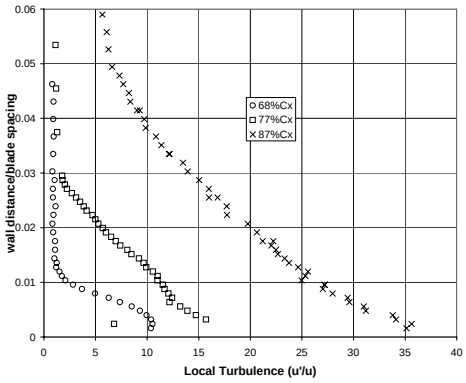

Figure 18. (a) Velocity boundary layer profiles for pulsed VGJ's. (b) Turbulence profiles for pulsed VGJs.

Continuous and Pulsed Vortex Generator Jets

In the same cascade, steady and pulsed vortex generator jets have been found to be extremely effective at reducing low Reynolds number separation. In the pulsed application, this was demonstrated even at very low duty cycles, as low as 1%. Recent PIV measurements on pulsed VGJ's by Johari and Rixon[52], has shown that the starting skew vortex penetrates 50% farther and has 30% higher peak vorticity than a steady jet with the same blowing ratio. The 90° skew cylindrical VGJ's (inclined at a 30° pitch angle) are located at two span wise locations, 45% and 63% chord. The VGJ diameter is 1mm with a pitch of 10d. Steady and pulsed blowing resulted in reattachment of the separated flow, for a wide range of blowing ratios, as is illustrated in Figure 15a.

For the unsteady experiments, a high speed solenoid valve manufactured by General Valve was pulsed at rates from 10 Hz to 100 Hz with a variable pulse width. The VGJ pulse shape measured at the VGJ exit by hot wire is shown in Figure 16 to be quite square and sharp as the duty cycle is reduced from 0.05 sec to 0.001 sec at 10 Hz.

The pulsed VGJ's showing a lower loss coefficient for very low mean blowing ratios. The performance of the steady flow VGJ's operated over a range of Re from 25K to 100K at a fixed blowing ratio of 2 show in Figure 15b a 50% reduced loss coefficient for the Tu=1% case and nearly the same improvement for the Tu= 4% case[53,54].

The cascade boundary layer shear layer instability frequency was found to be 100 Hz at separation, the reduced frequency for the passage flow was 13 Hz, at a Reynolds number of 25,000. The pulsing frequency of 10 Hz was chosen for this investigation as this yields a Strouhal number of approximately 1, as recommended by Wygnaski and Seifert,[26], Nagib et al.,[48], McManus et al.,[55], and others. This also means that the starting control vortex pulse is being convected over the surface with the same period as a passage disturbance or separated shear layer instability, (being close to $1/7^{th}$ of 100 Hz (15 Hz), and the passage reduced frequency of 13 Hz). Spectrums without control, with steady blowing, and with pulse blowing, are shown in Figure 17. The no blowing case shows small broad band energy from 2 to 15 Hertz and small peaks at 30 and 60 Hertz, the reduced frequency of the passage flow and the

shear layer instability. Steady blowing shows a flattening of the spectrum between 8 and 100 Hertz, a broad peak at 200 Hertz, and a sharp peak at 500 Hertz. The 500 Hz peak corresponds to the vortex shedding frequency of the free stream around the injected jet diameter. The pulsed spectrum is completely dominated by the pulsing frequency and its harmonic multiples with a flat segment between 5 and 25 Hertz. Yurchenko observed that higher frequencies (the 500 Hertz introduced by the VGJ's) or smaller wavelengths than the natural occurring instabilities are required for effective control. Fast rise time pulses, such as square wave pulses would satisfy this requirement by having a very broad frequency content. These square pulses should be treated differently than traditional instabilities and further computations and experiments are necessary to examine the interaction and contribution of the starting/stopping vortex more carefully.

The wall BL velocity and turbulence profiles with pulsed control show stable well behaved attached velocity profiles with monotonically increasing Tu levels in Figures 18a,b. The loss coefficient (obtained by integrating the velocity total pressure loss profile across the controlled passage and normalized by the integrated no control profile) is shown in Figure 19a as a function of duty cycle at 10Hz. The loss coefficient shows a reduction of 40-50 % and is nearly independent of the duty cycle down to 1% at a Re of 25K. The effect of the forcing frequency is illustrated in Figure 19b which shows the reduction in the loss coefficient ratio $\gamma_{int}/\gamma_{int0,}$ was 0.48, 0.46, and 0.44 at an effective blowing ratio of 0.4 for the pulsing introduced at the 63% C_x location at 10Hz, 50 Hz, and 100 Hz respectively. The duty cycle was 50% and Re 25,000 for these measurements. Above 100 Hz the pulse became sinusoidal and below 10 Hz the forcing frequency becomes less than the reduced frequency for the flow over the surface. Less than 10 Hz forcing resulted in a fluctuating separation and reattachment.

The stagger or pitch of the cascade was increased from design to determine if the flow could still be reattached and wake losses minimized for larger separations. Pitch was increased to: 1.25 x design, 1.5 x design, and 2 x design. The separation point was predicted by MISES and was found to move linearly upstream with pitch following the uncovered turning point. The separated profiles for the untreated blade are illustrated in Figure 20 and for VGJ's at 65% C_x, the reattached loss coefficients as a function of blowing ratio are showing Figure 21 to be capable of reattaching all pitches given sufficient VGJ blowing ratio.

Blade Profile and Total Inlet Pressure Measurements

Prediction of the accurate separation / reattachment locations that agree with experimental measurements turns out to be difficult for any existing computational approach as is illustrated by the abandonment of turbulence models producing some of the better overall results for comparison with low turbulence conditions. The inability of existing codes to accurately predict the separation location prompted accurate measurement of the blade profiles. Blade profiles were measured with 270 points evenly distributed around the pressure and suction surfaces with an additional 25 points each around the leading and trailing edges for >320 points overall. The cascade blades were profiled at, 1.4%, 39%, 49%, 61%, and 97% of span. The profile measurements are typically with in ± .25 mm of

the design profile as illustrated by the magnified profile section in Figure 22. Span wise measurements were also made at 1cm increments at 12 fixed span locations which indicated a constant value ±0.1 mm over the 89 mm span.

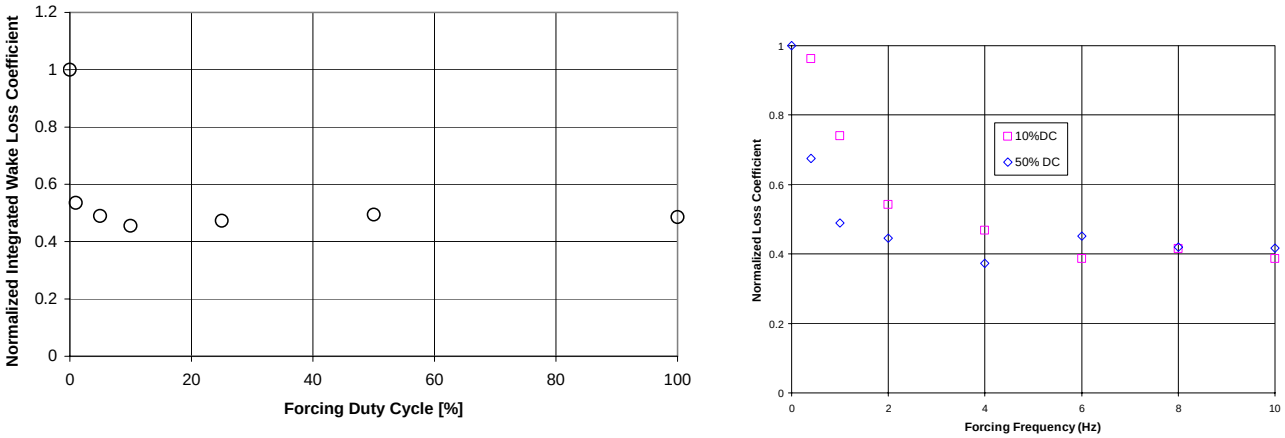

Figure 19. (a) Loss coefficient for pulsed VGJ's, Tu =1%, Re = 25,000. (b). Loss coefficient vs forcing f.

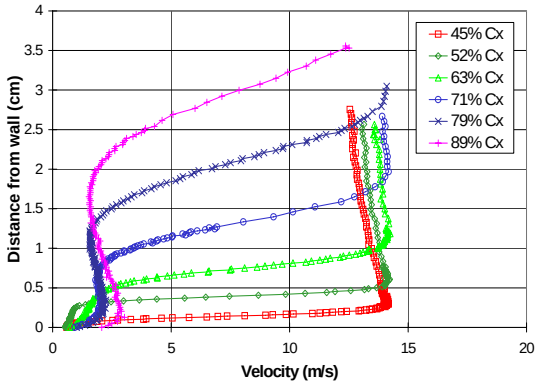

Figure 20. No control separated flows, pitch 1.5.

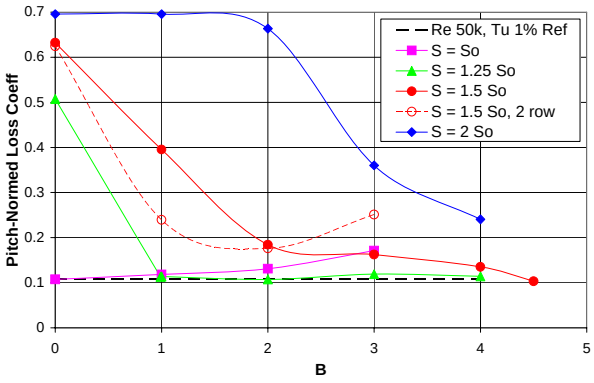

Figure 21. VGJ reattachment with increasing pitch, S.

A set of three actual HPT blades, Figure 23, were dimpled with a single row of suction surface dimples, just upstream of the uncovered turning, in a rainbow annular vane array. The vane wakes and the vane loss coefficients were compared to the untreated vanes on either side of the dimpled vanes in the Turbine Research Facility (TRF). The TRF is a matched parameter transient facility with a test time of ~3 seconds for low Reynolds numbers. A rake with nine total probes, located at the centers of equal area, is swept over the wakes of 11 vanes and the loss coefficient, γ, calculated. At this time the analysis of this data is incomplete. The application in a full scale rotating turbine still needs to be accomplished along with evaluation of the effects of combustion products.

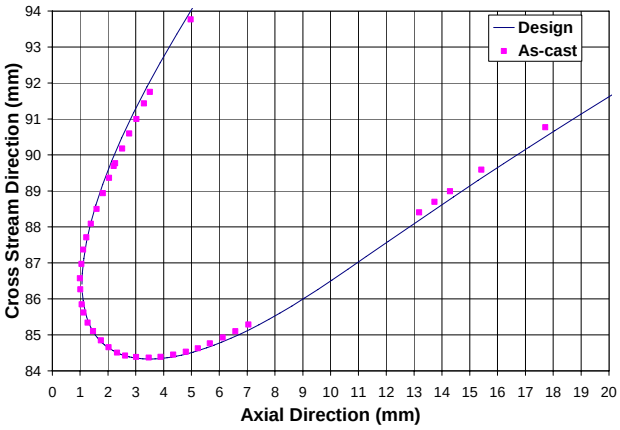

Figure 22. Design vs. as fabricated cascade profile < ±0.25mm.

Figure 23. Dimpled HP vanes.

SUMMARY

Longitudinal vortices have been introduced near the separation location on model LPTs by both dimples and VGJ's which effectively reduce separation losses at low Reynolds numbers by promotion of early transition, entrainment of high energy free stream flow, and the non steady starting/ stopping vortex.

Four dimple locations 50%, 55%, 65%, and 76% C_x and two VGJ locations 45% and 63% were evaluated showing that the location of separation treatment was not critical. Both VBI and MISES indicate initial separation to occur near the uncovered turning in contrast to an unbounded airfoil which separates near the leading edge. MISES was also used to predict the separation for the increased pitch study which again indicated a linear relationship with pitch or linear with uncovered turning. Experiment always indicates separation to occur near the uncovered turning point. The addition of a second row of dimples at 76% chord did not further reduce the loss coefficient. Increasing the dimple spacing on the original 65% C_x dimples by a factor of two to 4.44 cm did not adversely effect the loss coefficient reduction. VBI and MISES were both useful in predicting separation to be near the uncovered turning location. While computations still have a difficult time accurately predicting separation and reattachment very useful results were obtained to assist in optimization with Fluent predicting improved performance for the 4.44 cm dimple spacing by another 17% and indicating poorer performance of the half filled dimples. Although control is more effective for the treatment near the separation location, control is effective even if the separation location is not accurately known or predicted. The dimples showed a 45-50% reduction in loss coefficient at a Reynolds number of 25000 for turbulence levels of 1-4%. In addition a small reduction in loss is observed at higher Reynolds numbers. A dimple design for an actual LP Blade would require a dimple a few mm in diameter and 0.1 mm to 0.3 mm deep. A typical surface finish on newly manufactured blading is typically 1-2 μm. In- use LP centerline average roughness might typically be the order of 5-10μm, still better than an order of magnitude less than the dimple depressions. Dimples could be machined, cast, or coated. As a mature technology dimples are affordable, robust,

retrofitable, and manufacturable. They have been demonstrated at large scale, having significant overall benefits for low Reynolds number turbine applications.

Steady and pulsed vortex generator jets have also demonstrated the ability to effectively reattach separated flows. Steady blowing promotes rapid mixing and early transition within 25d of the VGJ injection site, reducing the separation loss coefficient by 60% at a Re of 25000, Tu=1% and 15-20% at a Tu=4%. Pulsed injection on the contrary never shows classical transition instabilities and the pulsing frequency and its multiples are found within and beyond the original the boundary layer (to 2δ at 96% C_x) indicating a very different physical mechanism of reattachment and control. Pulsed VGJ control down to 1% duty cycles demonstrates effective separation control reducing the loss coefficient by 45% at a Re=25000. Since the pulsed VGJ forcing frequency remains pervasive through out the boundary layer leading edge implementation should also be investigated along with the other unsteady turbine flow effects. Application of an effective pulsed vortex with a $C\mu$ of 0.0001 would require a very small amount of control flow. The range of control parameter space, a forcing frequency of 1-10x the reduced flow frequency, a wide range of effective blowing ratios or amplitude, 0.2-4.0, (boundary layer penetration depth or range of Mach number application), makes pulsed VGJ's an attractive separation control technique.

Although the effects of turbulence, horseshoe vortices, passage vortices, wakes and rotational effects have not yet been completely evaluated the pulsed VGJ's are clearly capable of reattaching separated flows over a wide range of the parameter space for the LPT application. The reattachment of the increased stagger configurations indicate a more aggressive loading should be possible with out incurring additional losses. In particular, successful operation down to duty cycles of 1% evokes the potential for extremely low values of control mass flow. The 1% duty cycle demonstrated would have an effective slot $c\mu$ of 0.00005 for the 1% duty cycle. For a number of LPT blading applications the dimples or pulsed VGJ's could provide a 4-6% recovery of LPT efficiency on existing engines for high altitude applications The application of separation control to new highly loaded LPT's driving high bypass fans can provide a means of further reducing LPT part count LPT weight.

REFERENCES

[1] Helton, D., private communication, 1997.

[2] Matsunuma, T., Abe, H., Tsutsui, Y., and Murata, K., "Characteristics of an Annular Turbine Cascade at Low ReynoldsNumbers", ASME 98-GT-518, 1998.

[3] Dorney, D. and Ashpis, D., "Study of Low Reynolds Number Effects on the Losses in Low-Pressure Turbine Blade Rows," *International Journal of Turbo and Jet Engines*, Vol 16, No. 2, 1999, pp. 91-106.

[4] Qiu, S. and Simon, T., "An Experimental Investigation of Transition as Applied to Low Pressure Turbine Suction Surface Flows", ASME 97-GT-455, 1997.

[5] Sohn, K., Shyne, R., and DeWitt, K., "Experimental Investigation of Boundary Layer Behavior in a Simulated Low Pressure Turbine", ASME 98-GT-034, 1998.

[6] Huang, P. and Xiong, G., Transition and Turbulence Modeling of Low Pressure Turbine Flows", AIAA 98-0339, 1998.

[7] Butler, R., Byerley, A., VanTreuren, K., and Baughn, J., "The Effect of Turbulence Length Scale on Low Pressure Turbine Blade Heat Transfer", Submitted to International Journal of Heat and Fluid Flow, 2000.

[8]Huanag , J., Corke, T., Thomas, F., "Separation Control over Low Pressure Turbine Blades," KJ 5, American Physical Society, November 2002.

[9] List J., Byerley, A., Mclaughlin, T., Van Dyken, B., "Using a Plasma Actuator to Control Laminar Separation on a Linear Cascade Turbine Blade," AIAA 2003-1026, January 2003**.**

[10] Hultgren, L S., and Ashpis, D.E., "Demonstration of Separation Delay with Glow-Discharge Plasma Actuators" AIAA 2003-1025, January 2003.

[13] Halstead, D., "Boundary Layer Development in Multi-Stage Low Pressure Turbines", PhD Dissertation Iowa State University, 1996.

[14]Halstead, D., Wisler, D., Okiishi, T., "Boundary Layer Development in Axial Compressors and Turbines – Part 3 of 4: LP Turbines", ASME 95-GT-463, 1995.

[15] Howell, R, Ramesh, O., and Hodson, H., "High Lift and Aft Loaded Profiles for Low Pressure Turbines", Munich, Germany, ASME 2000-GT-0261, 2000.

[16] Arts, T., and Colton T., "Investigation of a High Lift LP Turbine Blade submitted to Passing Wakes: Part 1 Profile Loss and Heat Transfer," GT2004-53768.

[17] Arts, T., and Colton T., "Investigation of a High Lift LP Turbine Blade submitted to Passing Wakes: Part 2 Boundary Layer Transition," GT2004-53768.

[18] Walsh, M., "Riblets," *Viscous Drag Reduction in Boundary Layers*, edited by, Bushnell and Hefner, Vol 123, 1990, pp. 203-261.

[19] Bearman, P. W., and Harvey, J. K., "Golf Ball Aerodynamics," *The Aeronautical Quarterly*, 27(2), 1976, pp112-122.

[20] Bearman, P. W., and Harvey, J. K., "Control of Circular Cylinder Flow by the Use of Dimples," *AIAA Journal*, 31(10), 1993, pp1753-1756.

[21] Mahmood, G., Hill, M., Nelson, D., "Local Heat Transfer and Flow Structure On and Above a Dimpled Surface in a Channel", ASME 2000-GT-230, 2000.

[22] Musiyenko,V. P., "Experimental study of the Flow Around Localized Deepenings", Bionics, ISSN 0374-6569, Nr. 26, 1993, pp. 31-34.

[23]Saric, W., Reed, H., Mehregany, M., and Reshotko, E., "Control of Transition in Swept-Wing Boundary Layers Using MEMS Devices as Distributed Roughness", AFOSR Contractor's Meeting on Turbulence and Internal Flows / Unsteady Aerodynamics, 1998, pp 361-366.

[24] Meyer, R., Bechert, D., Hage, W., and Montag P., "BMBF-Vorhaben,13N6537-Aeroflexible, Oberflachenklappenals "Ruckstrombremsen" nach dem Vorbild der Deckfedern des Vogelflugels," DLR IB 92517-97/B5, 1997.

[25] Lin, J.C., Howard, F.G., Bushnell, D.M., and Selby, G.V., "Investigation of Several Passive and Active Methods of Turbulent Flow Separation Control," AIAA 90-1598, 1990.

[26] Wygnanski I., and Seifert A., "The Control of Separation By Periodic Oscillations," AIAA 94-2608, 1994.

[27] Weaver, D., McAlister, K., and Tso, J., "Suppression of Dynamic Stall by Steady and Pulsed Upper-Surface Blowing", 1998, AIAA 98-2413.

[28]Wu, J., Lu, X., Denny, A., Fan, M., and Wu, J., "Post-Stall Flow Control on an Airfoil by Local Unsteady Forcing," *Journal of Fluid Mechanics*, Vol. 371, 1998, pp. 21-58.

[29] Yurchenko, N., and Rivir R. B., "Improvement of the Turbine Blade Performance Based on the Flow Instability and

Receptivity Analysis," Proceedings of the 8th International Symposium on Transport Phenomena and dynamics of Rotating Machinery Vol. 1, 2000, pp. 300-306.

[30] Glezer, A., "Shear Flow Control Using Synthetic Jet Fluidic Actuator Technology", AFOSR Contractor's Meeting on Turbulence and Internal Flows, 1997, pp 147-213.

[31] Amitay, M., Kibens, V., Parekh, D., and Glezer, A., "The Dynamics of Flow Reattachment over a Thick Airfoil Controlled by Synthetic Jet Actuators", AIAA-99-1001, 1999.

[32]McCormick, D., "Boundary Layer Separation Control with Directed Synthetic Jets", AIAA 2000-0519, 2000.

[33]Rediniotis, O., Lagoudas, D., and Wilson L., "Development of a Shape-Memory-Alloy Actuated Biomimetic Hydrofoil", AIAA 2000-0522.

[34]Velkoff, H., "Investigation of the Effects of Electro-static Fields on Heat Transfer and Boundary Layers", 1962, Dissertation 63-95.

[35] El-Khabiry, S. and Colver, G.M., "Drag reduction by DC Corona Discharge along an Electrically Conductive Flat Plate for Small Reynolds Number Flow," Physics of Fluids Vol. 9, No 3, March 1997, pp 587-599.

[36]Roth, J.R., Sherman, D.M., and Wilkinson, S.P., "Boundary Layer Flow Control with a One Atmosphere Uniform Glow Discharge Surface Plasma," AIAA 98-0328, January 1998.

[37]Corke, T.C., and Cavalieri, D.A., "Controlled Experiments on Instabilities and Transition to Turbulence in Supersonic Boundary Layers," AIAA 97-1817, July 1997.

[38] Rivir, Jacob, White, Carter, Ganguly Forelines, & Crafton, , “AC and Pulsed Plasma Flow Control,” AIAA 2004 -0847, Aerospace Sciences, Reno, January 2004.

[39] Driver, D., and Hebbar, S., “Experimental Study of a Three-Dimensional, Shear-Driven, Turbulent Boundary Layer,” AIAA Journal 25, 35, 1987.

[40]Jung, W., Mangiavacchi, N., and Akhaven, R., “Suppression of Turbulence in Wall-Bounded Flows by High-Frequency Spanwise Oscillations,” *Journal of Physics Fluids*, Vol. 4, No. 8, 1992, pp 1605 & 1606.

[41]Nagararaja K.S., “Advances in Ejector Technology – A Tribute to Hans Von Ohain’s Vision”, AFAPL-TR-79-2126, A Collection of Papers in Aerospace Sciences, 1982, pp. 490-517.

[42] Bechert, D., Bruse, M., Hage, W., and Meyer, R., “Biological Surfaces and their Technological Application -– Laboratory and Flight Experiments on Drag Reduction and Separation Control”, AIAA-97-1960, 1997.

[43]Maciejewski and Rivir, “Effects of Riblets and Free-Stream Turbulence on Heat Transfer in a Linear Turbine Cascade,” ASME 94-GT-245, 1994.

[44]Rothenflue, J.A. and King, P.I., "Vortex Development Over Flat Plate Riblets in a Transitioning Boundary Layer," *AIAA Journal*, Vol. 33, No. 8, 1995, pp. 1525-1526.

[45]Seifert, A., Bachar, T., Koss, D., Shepshelovich, M., and Wygnanski, I., “Oscillatory Blowing: A Tool to Delay Boundary-Layer Separation,” *AIAA Journal*, Vol. 31, No. 11, 1993, pp. 2052-2060.

[46] Smith, B. and Glezer A., “The Formation and Evolution of Synthetic Jets” *Physics of Fluids*, Vol. 10, No. 9, 1998, pp. 2281-2297.

[47] Fasel, H., “Control of Separation Using Pulsed Wall Jets: Numerical Investigations Using DNS and LES”, AFOSR Contractor’s Meeting on Turbulence and Internal Flows / Unsteady Aerodynamics and Hypersonics Con48, 1998.

[48] Nagib, H., Hites, M., Williams D., Wygnaski I., and Seifert, A., “Lift Enhancement Using Oscillatory Blowing at Compressible Flow Conditions,” AFOSR Contractor’s Meeting on Turbulence and Internal Flows / Unsteady Aerodynamics, 1998, pp 281-284.

[49] Lin, Y., Shih, T., and Chyu, M., “Computations of Flow and Heat Transfer in a Channel with Rows of Hemispherical Cavities”, ASME 99-GT-263, 1999.

[50]Lake, J., “Flow Separation Prevention on a Turbine Blade in Cascade at Low Reynolds Number”, PhD Dissertation, Air Force Institute of Technology, 1999.

[51] Koch , P. private communication, 2002.

[48] Rouser, K. P., “Use of Dimples to Suppress Boundary Layer Separation on a Low Pressure Turbine Blade,” AFIT MS Thesis, AFIT/GAE/ENY/02-13, December 2002.

[51] Casey, J.P., “Effect of Dimple Pattern on the Suppression of Boundary Layer Separation on a Low Pressure Turbine Blade,” AFIT MS Thesis, AFIT/GAE/ENY/04-M05, March 2004.

[52]Johari, H., and Rixon G.S., “Evolution of a Pulsed Vortex Generator Jet in a Turbulent Boundary Layer,” AIAA-2002-2834, 2002.

[53]Bons, J., Sondergaard, R., and Rivir, R., “Control of Low-Pressure Turbine Separation Using Vortex Generator Jets”, AIAA-99-0367, 1999.

[54] Bons, J., Sondergaard, R., and Rivir, R., “Turbine Separation Control Using Pulsed Vortex Generator Jets”, ASME 2000-GT-262, 2000.

[55] McManus, K., Legner, H., and Davis, S., “Pulsed Vortex Generator Jets for Active Control of Flow Separation,” AIAA -94-2218, 1994.

[56]Johari, H., and McManus, K., “Visualization of Pulsed Vortex Generator Jets for Active Control of Boundary Layer Separation,” AIAA-97-2021, 1997.

NOMENCLATURE

B = jet blowing ratio = $(\rho u)_{jet}/(\rho u)_{local}$

c_p = pressure coefficient = $(p_{T,in}-p_{S,local})/(p_{T,in}-p_{S,in})$

C_x = blade axial chord (0.18m)

C_μ = steady blowing coefficient = $\rho U_j^2 / \frac{1}{2}\rho U_{\infty j}^2$

d = jet hole diameter (1mm)

f = forcing frequency [Hz]

F+= dimensionless pulsing frequency= fL_f/U_∞

L_f = length, flap length or c for airfoil (m)

p = pressure [Pa]

R = radius of curvature (m)

Re = inlet Reynolds number = $\rho_{in} u_{in} C_x/\mu$

Tu = turbulence level (u'/ u) in percent [%]

U or u = stream wise mean velocity [m/s]

u' = stream wise rms fluctuating velocity [m/s]

u_τ = wall shear velocity (m/sec)

δ = boundary layer thickness

μ = dynamic viscosity

ν = kinematic viscosity = μ/ρ

γ = wake loss coefficient = $(p_{T,in}-p_{T,ex})/(p_{T,in}-p_{S,in})$

$$\gamma_{int} = \int_{-wake/2}^{+wake/2} \left(\frac{P_{T,in} - P_{T,ex}}{P_{T,in} - P_{S,in}} \right) dy$$ integrated wake loss coefficient

Λ_0 = non dimensional wavelength= $\lambda_z^{3/2} U_0/\nu R^{1/2}$

λ_z = span wise scale (diameter) (mm)

ρ = density (kg/m3)